Cellular/Molecular

Ca^{2+}-Dependent Regulation of Ca^{2+} Currents in Rat Primary Afferent Neurons: Role of CaMKII and the Effect of Injury

Qingbo Tang,[1] Madhavi Latha Yadav Bangaru,[1] Sandra Kostic,[1] Bin Pan,[1] Hsiang-En Wu,[1] Andrew S. Koopmeiners,[1] Hongwei Yu,[1] Gregory J. Fischer,[1] J. Bruce McCallum,[1] Wai-Meng Kwok,[1] Andy Hudmon,[2] and Quinn H. Hogan[1,3]

[1]Medical College of Wisconsin, Department of Anesthesiology, Milwaukee, Wisconsin 53226, [2]Indiana University School of Medicine, Department of Biochemistry and Molecular Biology-Stark Neuroscience Research Institute, Indianapolis, IN 46202, [3]Zablocki VA Medical Center, Milwaukee, Wisconsin 53295

Currents through voltage-gated Ca^{2+} channels (I_{Ca}) may be regulated by cytoplasmic Ca^{2+} levels ($[Ca^{2+}]_c$), producing Ca^{2+}-dependent inactivation (CDI) or facilitation (CDF). Since I_{Ca} regulates sensory neuron excitability, altered CDI or CDF could contribute to pain generation after peripheral nerve injury. We explored this by manipulating $[Ca^{2+}]_c$ while recording I_{Ca} in rat sensory neurons. In uninjured neurons, elevating $[Ca^{2+}]_c$ with a conditioning prepulse (−15 mV, 2 s) inactivated I_{Ca} measured during subsequent test pulses (−15 mV, 5 ms). This inactivation was Ca^{2+}-dependent (CDI), since it was decreased with elimination of Ca^{2+} influx by depolarization to above the I_{Ca} reversal potential, with high intracellular Ca^{2+} buffering (EGTA 10 mM or BAPTA 20 mM), and with substitution of Ba^{2+} for extracellular Ca^{2+}, revealing a residual voltage-dependent inactivation. At longer latencies after conditioning (>6 s), I_{Ca} recovered beyond baseline. This facilitation also proved to be Ca^{2+}-dependent (CDF) using the protocols limiting cytoplasmic Ca^{2+} elevation. Ca^{2+}/calmodulin-dependent protein kinase II (CaMKII) blockers applied by bath (KN-93, myristoyl-AIP) or expressed selectively in the sensory neurons (AIP) reduced CDF, unlike their inactive analogues. Protein kinase C inhibition (chelerythrine) had no effect. Selective blockade of N-type Ca^{2+} channels eliminated CDF, whereas L-type channel blockade had no effect. Following nerve injury, CDI was unaffected, but CDF was eliminated in axotomized neurons. Excitability of sensory neurons in intact ganglia from control animals was diminished after a similar conditioning pulse, but this regulation was eliminated by injury. These findings indicate that I_{Ca} in sensory neurons is subject to both CDI and CDF, and that hyperexcitability following injury-induced loss of CDF may result from diminished CaMKII activity.

Introduction

Key functions in excitable cells are regulated by cytoplasmic Ca^{2+} levels ($[Ca^{2+}]_c$), such as contraction in myocytes and excitation and synaptic transmission in neurons (Berridge et al., 2000). This critical signal is shaped by powerful feedback control of Ca^{2+} entry through voltage-gated Ca^{2+} channels (VGCCs), where two phenomena with opposing effects on $[Ca^{2+}]_c$ have been identified. Ca^{2+}-dependent inactivation (CDI) is evident for various VGCC subtypes in myocytes (Hadley and Lederer, 1991) and neurons (Cox and Dunlap, 1994; Forsythe et al., 1998; Meuth et al., 2002), while Ca^{2+}-dependent facilitation (CDF) has been demonstrated for L-type VGCC in myocytes (Anderson et al., 1994; Yuan and Bers, 1994) and for P/Q channels in neurons of the CNS (Borst and Sakmann, 1998; Cuttle et al., 1998; Chaudhuri et al., 2005).

The molecular mechanism underlying CDI requires binding of Ca^{2+} to pre-associated calmodulin (CaM), a process conserved in all VGCCs (Zühlke et al., 1999; Pitt et al., 2001; Liang et al., 2003). A similar direct action of CaM may produce CDF in L-type and P/Q-type channels (Lee et al., 1999; DeMaria et al., 2001; Liang et al., 2003). However, other studies implicate the participation of the serine/threonine protein kinase, Ca^{2+}/calmodulin-dependent protein kinase II (CaMKII) (Yuan and Bers, 1994; Dzhura et al., 2000), leading to binding or phosphorylation of channel targets including the pore-forming α-subunits of VGCCs (Hudmon et al., 2005; Jiang et al., 2008; Blaich et al., 2010) and the auxiliary β-subunits (Grueter et al., 2006). CaMKII contribution to the production of CDF has been implicated for both L-type and P/Q-type channels (Hudmon et al., 2005; Jiang et al., 2008), but not for N-type channels, nor for any VGCC in the peripheral nervous system.

Neuronal activity is regulated by Ca^{2+} entering through VGCCs, which in turn activates Ca^{2+}-sensitive K^+ currents and thereby provides a critical brake on neuronal depolarization and action potential (AP) generation (Swensen and Bean, 2003; Hogan et al., 2008; Lirk et al., 2008; Gemes et al., 2009). Painful

Received Feb. 27, 2012; revised June 25, 2012; accepted July 5, 2012.

Author contributions: Q.T., M.L.Y.B., W.-M.K., A.H., and Q.H.H. designed research; Q.T., M.L.Y.B., S.K., B.P., H.-E.W., A.S.K., H.Y., G.J.F., J.B.M., and Q.H.H. performed research; Q.T., M.L.Y.B., S.K., B.P., H.-E.W., A.S.K., H.Y., W.-M.K., A.H., and Q.H.H. analyzed data; Q.T., M.L.Y.B., H.Y., A.H., and Q.H.H. wrote the paper.

This work was supported by National Institutes of Health Grants NS-42150 (Q.H.H.) and DA-K01 02475 (H.-E.W.).

The authors declare no competing financial interests.

Correspondence should be addressed to Dr. Quinn H. Hogan, Medical College of Wisconsin, Department of Anesthesiology, 8701 Watertown Plank Road, Milwaukee, WI 53226. E-mail: qhogan@mcw.edu.

DOI:10.1523/JNEUROSCI.0983-12.2012

 0270-6474/12/3211737-13$15.00/0

nerve injury results in diminished I_{Ca} in sensory neurons (Baccei and Kocsis, 2000; Abdulla and Smith, 2001; McCallum et al., 2006, 2011) and reduced activity-induced cytoplasmic Ca^{2+} accumulation (Fuchs et al., 2007a,b; Gemes et al., 2010), which lead to enhanced sensory neuron excitability (Sapunar et al., 2005). Although the mechanism of this loss in VGCC function could involve multiple levels of regulation, we pursued the hypothesis that injury disrupts Ca^{2+}-dependent modulation (CDI and/or CDF) of VGCCs—a model consistent with our observation of diminished levels of cytoplasmic Ca^{2+} and activated CaMKII in injured sensory neurons (Kojundzic et al., 2010). Accordingly, this study was designed to examine CDI and CDF in the natural physiological context of sensory neurons, to identify the influences of injury and CaMKII signaling, and to identify whether this regulation plays a role in controlling neuronal excitability.

Materials and Methods

Ethical approval. Prior approval and ongoing oversight for the studies described below were provided by the Medical College of Wisconsin Animal Care and Use Committee. The animals were cared for in a facility accredited by the Association for Assessment and Accreditation of Laboratory Animal Care International, registered with the United States Department of Agriculture, and compliant with United States Public Health Service regulations and requirements and provisions of the Animal Welfare Act.

Animal preparation. One hundred thirty-four unoperated male Sprague Dawley rats (Taconic) weighing 125–150 g were used for these experiments. Other rats ($n = 37$) were subjected to spinal nerve ligation (SNL), based on the method of Kim and Chung (1992). Briefly, during anesthesia by inhalation of isoflurane (1.5–2.5% in oxygen) without neuromuscular blockade, the right lumbar paravertebral region was exposed through a midline incision, and the sixth lumbar (L6) transverse process was removed to expose the L5 and L6 spinal nerves, which were ligated with 4-0 silk suture and sectioned ~5 mm distal to their respective dorsal root ganglia (DRGs). The wounds were closed in layers and the skin stapled. Control rats received skin incision and closure only.

Sensory testing. Rats underwent sensory testing for a form of hyperalgesic behavior that we have previously documented to be associated with an aversive percept (Hogan et al., 2004; Wu et al., 2010). Briefly, on three different days between 10 and 21 d after surgery, right plantar skin was mechanically stimulated with a 22G spinal needle with adequate pressure to indent but not penetrate the skin. Whereas control animals respond with only a brief reflexive withdrawal, rats following SNL may display a complex hyperalgesia response that incorporates sustained licking, chewing, grooming, and sustained elevation of the paw. The frequency of hyperalgesia responses was tabulated for each rat.

Dissociation of DRG neurons. Between 21 and 30 d postsurgery, L5 DRGs from control or SNL rats were removed following decapitation under deep isoflurane anesthesia. In some cases, L4 DRGs from control animals were also used since there are no evident differences between them in the uninjured state. Ganglia were placed in a 35 mm dish containing Ca^{2+}/Mg^{2+}-free, cold HBBS (Life Technologies) and cut into four to six pieces that were incubated in 0.5 mg/ml liberase TM (Roche) in DMEM/F12 with glutaMAX (Life Technologies) for 30 min at 37°C followed with 1 mg/ml trypsin (Sigma-Aldrich) and 0.36 mg/ml DNase (Sigma-Aldrich) for another 10 min. After addition of trypsin inhibitor (type II; Sigma-Aldrich), tissues were centrifuged and lightly triturated in neural basal media (1×) (Life Technologies) containing 2% (v:v) B27 supplement (50×) (Life Technologies), 0.5 mM glutamine (Sigma-Aldrich), 0.05 mg/ml gentamicin (Life Technologies), and 10 ng/ml nerve growth factor 7S (Alomone Labs Ltd.). Cells were then plated onto poly-L-lysine (70–150 kDa; Sigma-Aldrich)-coated coverslips and cultured at 37°C in 5% CO_2. All cells were studied 3–8 h after dissociation. Small- to medium-sized (30 ± 3 μm) neurons were used for this study.

Whole-cell patch-clamp recording. Electrodes with a resistance of 2–4MΩ were pulled from borosilicate glass (Garner Glass) using a micropipette puller (P-97; Sutter Instrument) and fire polished. Recording was performed in the whole-cell configuration with an Axopatch 200B amplifier (Molecular Devices). After whole-cell configuration was established, electrical compensation for the cell membrane capacitance and series resistance were initiated. Neurons with >10 MΩ access resistance after breakthrough were discarded. Experiments were performed 5–15 min after breakthrough, and at room temperature (~25°C). Signals were filtered at 2 kHz through a 4-pole Bessel filter, and digitized at 10 kHz with a Digidata 1320 A/D interface (Molecular Devices).

Seals were achieved in modified Tyrode's containing (in mM): 140 NaCl, 4 KCl, 2 $CaCl_2$, 2 $MgCl_2$, 10 D-glucose, and 10 HEPES, pH of 7.4, with an osmolarity of 300 mOsm. Voltage-induced currents flowing through Ca^{2+} channels were recorded using an extracellular solution containing (in mM): 2 $CaCl_2$ or 2 $BaCl_2$, 4-aminophyridine 1, 10 HEPES, 140 tetraethylammonium chloride (TEACl), pH of 7.4, with an osmolarity of 300 mOsm. The internal pipette solution contained (in mM): 120 CsCl, 10 TEACl, 4 Mg-ATP, 0.3 Na-GTP, 0.5 EGTA, 0.2 $CaCl_2$, 1 $MgCl_2$, and 10 HEPES, pH of 7.2, with an osmolarity of 300 mOsm. The free concentration for Ca^{2+} was calculated to be 90 nM using Maxchelator (http://maxchelator.stanford.edu). Measured voltages are corrected for the junction potential (−5 mV). Data from whole-cell I_{Ca} recordings were evaluated with Axograph X 1.3.5 (AxoGraph Scientific), with which peak inward currents and charge transfer were measured. To correct for cell size, inward currents are expressed as a function of cell capacitance (pA/pF).

Intracellular recording. Intact ganglia with dorsal roots attached were harvested by laminectomy during isoflurane anesthesia and placed in artificial CSF containing (in mM): 128 NaCl, 3.5 KCl, 1.2 $MgCl_2$, 2.3 $CaCl_2$, 1.2 NaH_2PO_4, 24.0 $NaHCO_3$, and 11.0 glucose bubbled by 5% CO_2 and 95% O_2 to maintain a pH of 7.35. Intracellular recordings were performed with microelectrodes fashioned from borosilicate glass (1mm OD, 0.5 mm ID, with Omega fiber) (FHC Bowdoinham) using a P-97 programmable micropipette puller (Sutter Instrument). Pipettes were filled with 2M K^+ acetate, which was buffered with 10 mM HEPES, with a resulting resistance of 60–90 MΩ. Neurons were impaled using differential interference contrast imaging and infrared illumination. Membrane potential was recorded using an active bridge amplifier (Axoclamp 2B; Molecular Devices). Voltage recordings were filtered at 10 kHz and then digitized at 40 kHz (Digidata 1322A; Molecular Devices) and analyzed off-line (AxoGraph X 1.3.5; AxoGraph Scientific). Recordings were not started until resting membrane potential had stabilized (typically within 2 min), at which time neurons were excluded if the resting membrane potential was less polarized than −45 mV. Somatic APs were generated by direct membrane depolarization with current injection through the recording electrode, for which voltage error was minimized using a discontinuous current-clamp mode with a switching rate of 2 kHz, while monitoring for complete settling of electrode potential between sampling. Excitability was assayed by counting the number of APs generated by injection of depolarizing current through the recording electrode (2 nA, 50 ms). This stimulus produced repetitive firing in approximately half of the neurons. A conditioning prepulse was produced during single-electrode voltage-clamp (0 mV, 2 s) from a holding potential that was identical to the cell's resting membrane potential, after which the recording mode was automatically switched to discontinuous current-clamp mode for determining firing pattern during subsequent test pulses (2 nA, 50 ms). Data were included only from neurons that showed depolarization to 30 mV or less.

Cytoplasmic Ca^{2+} microfluorometry. Fura-2 (pentapotassium salt from Invitrogen) was dissolved in H_2O to a concentration of 10 mM, and then diluted to 200 μM in internal pipette solution for whole-cell patch-clamp recordings. Experiments were started 5–10 min after the whole-cell configuration was established, during which loading was achieved by passive diffusion. The fluorophore was excited alternately with 340and 380 nm wavelength illumination (150W Xenon, Lambda DG-4; Sutter Instrument), while images were acquired at 510 nm using a cooled 12-bit digital camera (Coolsnap fx; Photometrics). Images were obtained using an inverted microscope (Diaphot 200; Nikon Instruments) and a 40× fluor oil-immersion objective. The ratio of fluorescence emission during 340 nm excitation divided by the intensity during 380 nm excitation ($R_{340/380}$) was calculated as an indicator of $[Ca^{2+}]_c$. This ratio was calculated on a

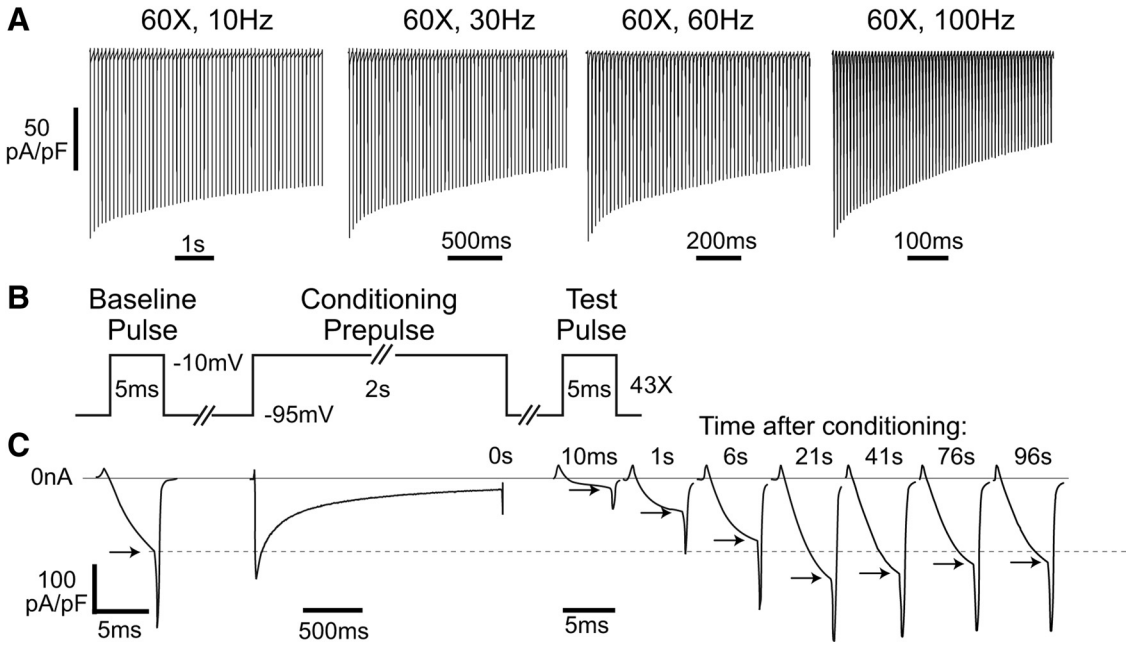

Figure 1. Ca^{2+} current changes during pulse trains and in response to a prior conditioning prepulse. ***A***, Currents elicited by trains of 60 AP waveform voltage commands at 10, 30, 60, and 100 Hz show progressive inactivation and no net facilitation. Note different time scales for each trace. ***B***, After a sustained conditioning prepulse (2 s depolarization to −10 mV), test depolarizations (5 ms duration, −10 mV; at 10 ms, 100 ms, 300 ms, and 1 s, and every 2.5–98.5 s following the conditioning prepulse, not all are shown) produce currents (***C***) demonstrating initial net I_{Ca} inactivation of peak current (arrows) followed by net facilitation compared with the baseline I_{Ca} (dashed line).

pixel-by-pixel basis following background subtraction (MetaFluor; Molecular Devices).

Agents. Stock solutions were prepared by dissolving agents in either distilled water or dimethylsulfoxide (DMSO), at concentrations at least 1000 times the final concentration, and kept frozen in aliquots. The stock solutions were diluted in extracellular solution just before use. Solutions were delivered by gravity or through a pressure regulated microperfusion system (ALA-BP8 system; ALA Scientific) for at least 3 min before recording. Peptides were delivered in an external Ca^{2+} solution to which cytochrome *c* (0.1 mg/ml; Sigma-Aldrich) had been added to prevent nonspecific binding in the delivery system. This concentration has been shown to have no effect on I_{Ca} in cerebellar neurons (Randall and Tsien, 1995) and in sensory neurons (data not shown). KN-93, KN-92, chelerythrine, and dantrolene were purchased from EMD4 Biosciences. Nisoldipine and ω-conotoxin GVIA were purchased from Sigma-Aldrich. Myristoylated autocamtide-2-related inhibitory peptide (mAIP) was obtained from Alexis Bioscience. Effective concentrations of ω-conotoxin GVIA, nisoldipine, and dantrolene were based on prior findings in identical sensory neuron preparations (Gemes et al., 2009; McCallum et al., 2011).

Recombinant adeno-associated virus vectors. To construct the recombinant adeno-associated virus (rAAV) vector encoding a chimeric EGFP-AIP, a DNA fragment containing the EGFP-AIP sequence from pEGFPc1-AIP (kindly provided by Dr. Steven H. Green, Department of Biological Sciences, University of Iowa) (Bok et al., 2007; Zha et al., 2009) was cloned into the NdeI/HpaI sites of pAAV-DS-CMV, a double-strand (ds) AAV plasmid (Viromics), to generate pdsAAV-CMV-EGFP-AIP. EGFP released from pEGFP-c1 was cloned into pAAV-DS-CMV to generate pdsAAV-CMV-EGFP. The AAV vectors of AAV8-EGFP-AIP and AAV8-EGFP were produced in our laboratory by the triple transfection of either pdsAAV-CMV-EGFP-AIP or pdsAAV8-CMV-GFP (control) with pRC8 and pHelpler (Viromics) into 293T cells, followed by two cycles of cesium chloride gradient purification and concentrated as previously described (Grimm et al., 2003). Encapsidated DNA was quantified by a PicoGreen assay (Invitrogen) following denaturation of the AAV particles, and the physical titer was calculated and expressed as genome copy number per milliliter (GC/ml). The titers of AAV8-EGFP-AIP and AAV8-CMV-EGFP were 3.04×10^{12} GC/ml and 9.84×10^{12} GC/ml, respectively. All vector injections were 2 μl for each DRG, using an established technique (Fischer et al., 2011).

Statistical analysis. For comparisons between groups, matched recordings were used in which neurons from the same dissociations were mixed among the different groups. Unpaired *t* tests were performed between groups using Excel (Microsoft). One-way or two-way ANOVA was performed where appropriate and *post hoc* paired comparisons (Tukey's HSD) were performed using Prism (GraphPad Software). Comparisons of ratios of APs generated before and after conditioning in intact DRGs were compared with Mann–Whitney *U* test with Bonferroni correction for multiple comparisons. Data are presented as average ± SEM.

Results

Identification of CDI and CDF in sensory neurons

To explore whether I_{Ca} in sensory neurons is regulated by neuronal activity, we first used a simple repetitive pulse protocol that has been used to reveal inhibition and facilitation in various other cell types (DeMaria et al., 2001; Grueter et al., 2006; Blaich et al., 2010). Only a monotonic decrement in I_{Ca} was observed during stimulation at rates from 10–100 Hz ($n = 6$; Fig. 1*A*). While this pattern indicates a dominant effect of CDI and voltage-dependent inactivation (VDI) during tonic firing, it does not necessarily demonstrate the absence of CDF, which may be masked by concurrent CDI (Zühlke et al., 2000). Also, phasic activity may be a more relevant model of normal function in sensory neurons, which are quiescent apart from trains induced by receptive field stimulation (Ma et al., 2003). We therefore examined an alternative approach in which CDF is evaluated during recovery from a prior conditioning prepulse (Lee et al., 2000; Hudmon et al., 2005). A protocol was designed (hereafter referred to as the standard protocol; Fig. 1*B*,*C*) in which the holding potential was set at −95 mV to minimize preferential closed-state inactivation of Ca^{2+} channels (Patil et al., 1998). The duration of the test pulse was set at 5 ms to approximate the duration of an AP under patch recording conditions, and

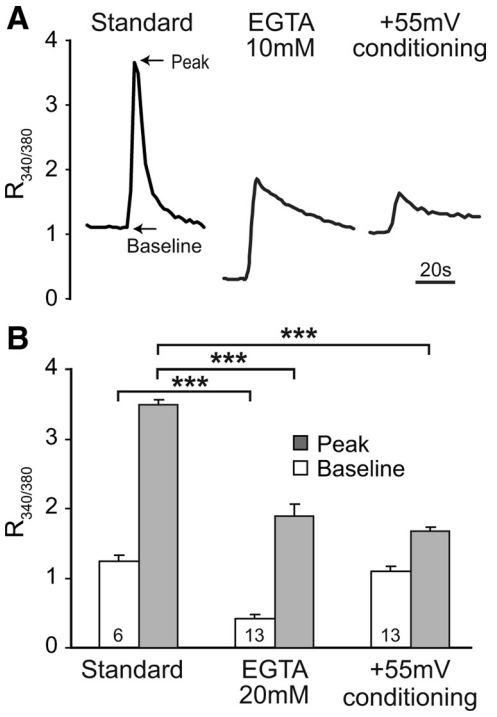

Figure 2. Cytoplasmic Ca^{2+} transients evoked by test protocols. ***A***, The standard protocol (prepulse depolarization to −10 mV for 2 s, pipette EGTA 0.5 mM, left trace) shows elevation of Fura-2 ratio of emission during excitation at 340 and 380 nm ($R_{340/380}$), which reflects cytoplasmic Ca^{2+} concentration. Recovery occurred despite the continuing train of test depolarizations (5 ms, −10 mV) every 2.5 s for 98.5 s. Increasing pipette EGTA (10 mM, middle trace) reduced the resting $[Ca^{2+}]_c$ and the transient peak. Prepulse depolarization to +55 mV with standard pipette EGTA (0.5 mM, right trace) selectively reduced transient peak, with a residual transient possibly due to the tail current during repolarization. Recordings were made 5–8 min after whole-cell configurations were established. ***B***, Summary data for baseline and peak $[Ca^{2+}]_c$ (arrows, ***A***) represented by fluorescence ratio. Mean ± SEM. Numbers in the bars indicate *n* for neurons of each group. Brackets indicate significant differences. ***$p < 0.001$. Baseline versus peak is also significantly different for each group.

the voltage was stepped to −10 mV, which is between the voltages producing peak current in Ba^{2+} and Ca^{2+} (Hogan et al., 2000; McCallum et al., 2006). Immediately (10 ms) following a conditioning prepulse (2 s depolarization to −10 mV), I_{Ca} showed an initial phase of net I_{Ca} inactivation (16 ± 1% of baseline, $n = 42$) that was followed by recovery. A delayed phase ensued during which I_{Ca} exceeded baseline (123 ± 4% at 22 ± 1 s). In additional matched groups of neurons, shorter conditioning prepulses also produced net facilitation (I_{Ca} peaks at 115 ± 6% of baseline for 250 ms of conditioning, $n = 4$; 118 ± 4%, for 500 ms, $n = 5$; 131 ± 5%, for 2 s depolarization, $n = 5$). Like I_{Ca} from myocytes and CNS neurons, these findings demonstrate activity-dependent modulation of I_{Ca} in sensory neurons.

To isolate Ca^{2+}-dependent influences (CDI and CDF), we used a reference protocol in which Ca^{2+} entry during the conditioning prepulse was prevented by depolarization to +55 mV, which is above the I_{Ca} reversal potential in these neurons (49.4 ± 1.4 mV, $n = 13$). This protocol restricts Ca^{2+} influx (Fig. 2) without affecting resting $[Ca^{2+}]_c$, and retains the influences of VDI and the repeated test pulses. In contrast to the standard protocol, depolarization to +55 mV was followed by initial I_{Ca} inhibition (VDI) but no facilitation phase (Fig. 3*A*). This clearly demonstrates the dependence of facilitation upon Ca^{2+} influx, and provides a reference for selective quantification of CDI and CDF in neurons recovering from a conditioning Ca^{2+} influx. Specifically (Fig. 3*B*), the difference at the 10 ms time point (termed %CDI) represents the maximal extent of net CDI, whereas the difference when the recovery curve maximally exceeds the +55 mV control curve (termed %CDF) represents the greatest extent of net CDF.

Characterization of CDI and CDF in sensory neurons

I_{Ca} amplitude during a test pulse immediately after the conditioning prepulse was reduced to 16 ± 1% of baseline (i.e., 84% total inactivation). The measured %CDI of 33 ± 2% ($n = 8$; Fig. 3*C*) indicates that most inactivation following depolarization under standard conditions is attributable to VDI. After recovery from inactivation, the large ensuing %CDF (34 ± 4%; Fig. 3*C*) identifies CDF as a powerful facilitatory influence in sensory neurons. We further examined the central question of Ca^{2+} dependence by replacing extracellular Ca^{2+} with Ba^{2+} as the charge carrier. This decreased CDI and prevented the development of CDF after neuronal activation (Fig. 3*C*,*D*). Delayed recovery of I_{Ca} was observed in Ba^{2+} bath solution, probably due to the accumulation of massive cytoplasmic Ba^{2+} loads secondary to the inability of the plasma membrane Ca^{2+}-ATPase to extrude Ba^{2+} (Mironov and Juri, 1990). Eliminating Ca^{2+} accumulation by buffering the Ca^{2+} influx with high pipette concentrations of either EGTA (10 mM), or the more rapid Ca^{2+} chelator BAPTA (20 mM) (Anderson et al., 1998; Lee et al., 2009), limited the global rise in $[Ca^{2+}]_c$ during the conditioning depolarization (Fig. 2) and decreased %CDI and %CDF (Fig. 3*C*,*D*), suggesting that a global increase in $[Ca^{2+}]_c$ rather than a local source drives activity-related inhibition and facilitation of VGCCs in sensory neurons.

The 5 ms duration of the test pulses did not allow I_{Ca} to reach its peak for every neuron (e.g., Fig. 1*C*). Thus, it is possible that facilitation of I_{Ca} recorded in this way represents either increased channel conductance or accelerated channel activation, as has been noted in heterologously expressed P/Q-type channels (Liang et al., 2003). To resolve which fundamental mechanisms contribute to CDF in sensory neurons, we used a modified protocol in which the standard conditioning prepulse was followed 20 s later by a test pulse that was sustained for 50 ms to also allow evaluation of peak I_{Ca} (Fig. 4*A*). The rate of I_{Ca} activation, determined by measuring the time to achieve peak current, was increased after conditioning (7.2 ± 0.8 ms vs 8.1 ± 0.7 ms at baseline, $n = 12$, $p < 0.01$; Fig. 4*B*). This observation confirms more rapid channel opening after conditioning, which may be particularly relevant to neuron function due to the brief duration of APs. Since peak I_{Ca} in this experiment was also increased (119 ± 20 pA/pF vs 100 ± 18 pA/pF at baseline, $n = 12$, $p < 0.001$), altered channel-gating kinetics and peak conductance operate in combination to produce CDF in sensory neurons. The persistence of CDF in this protocol in the absence of repetitive test pulses (%CDF is 21 ± 6%, $n = 12$, when I_{Ca} is measured 5 ms after test pulse initiation, normalized against an identical protocol, but with a conditioning prepulse to +55 mV, $n = 14$) indicates that latent CDF persists in a quiescent neuron after intense activity.

CDF outlasts elevated $[Ca^{2+}]_c$

Transient increase of $[Ca^{2+}]_c$ may act through acute signaling mechanisms directly coupled to $[Ca^{2+}]_c$, or may have more sustained consequences via post-translational modifications of proteins that persist beyond the return of $[Ca^{2+}]_c$ to baseline. To determine the temporal relationship between the clearance of cytoplasmic Ca^{2+} and Ca^{2+}-dependent changes in I_{Ca}, we fluo-

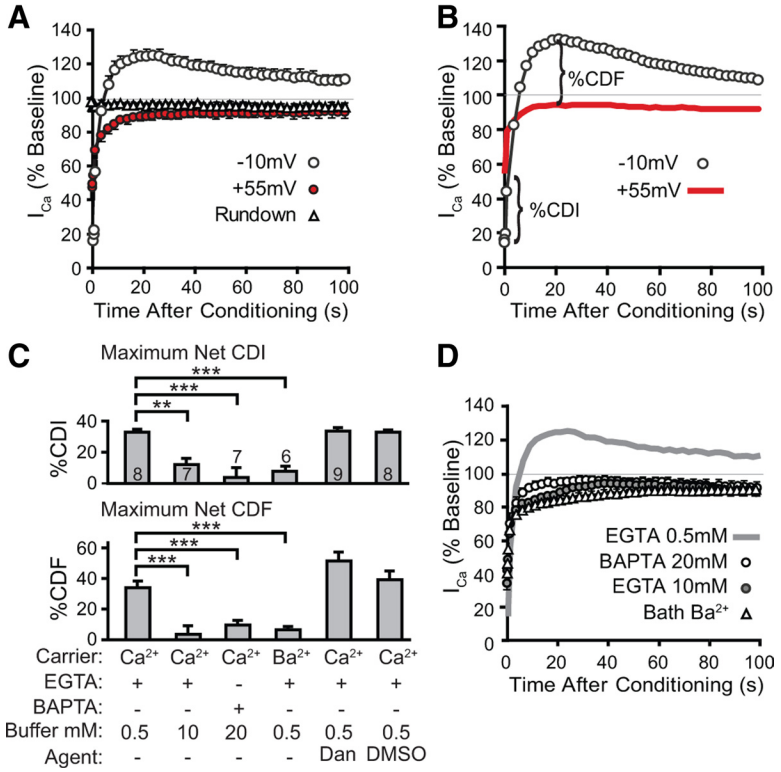

Figure 3. Effects of a conditioning prepulse on I_{Ca}. ***A***, Patterns of I_{Ca} recovery are affected by protocol conditions. The standard protocol (Ca^{2+} bath, pipette EGTA 0.5 mM, 2 s conditioning prepulse to −10 mV; $n = 8$) produced rapid initial inactivation of I_{Ca} and subsequent sustained facilitation of I_{Ca} above baseline. Depolarization to +55 mV during prepulse conditioning ($n = 7$) results in less initial inactivation and no facilitation. Without the conditioning prepulse (Rundown, $n = 10$), I_{Ca} induced by sequential test pulses developed minor rundown to 95 ± 2% of baseline, similar to the decrease observed at the end of the protocol using a +55 mV conditioning prepulse. ***B***, Defined parameters (%CDI, %CDF) are demonstrated for a sample recovery curve by comparing to the averaged recovery curve for the +55 mV protocol ($n = 12$ neurons). ***C***, Summary data for CDI and CDF. Protocols are specified according to their charge carrier (Ca^{2+} or Ba^{2+}), pipette solution buffer (EGTA or BAPTA), and buffer concentration. Dantrolene (Dan, 10 μM) was compared with its vehicle (DMSO). Mean ± SEM. Numbers in the bars indicate *n* for neurons of each group. Brackets indicate significant differences from the control condition (Ca^{2+} charge carrier, 0.5 mM EGTA): $^{*}p < 0.05$, $^{**}p < 0.01$, $^{***}p < 0.001$. ***D***, Compared with the standard 0.5 mM EGTA pipette buffering (gray line, same data shown for −10 mV in ***A***), replacing bath Ca^{2+} with Ba^{2+} as the charge carrier for I_{Ca} ($n = 6$), increasing pipette EGTA (10 mM, $n = 7$) or replacing it with BAPTA (20 mM, $n = 7$) reduces initial inactivation and eliminates subsequent facilitation.

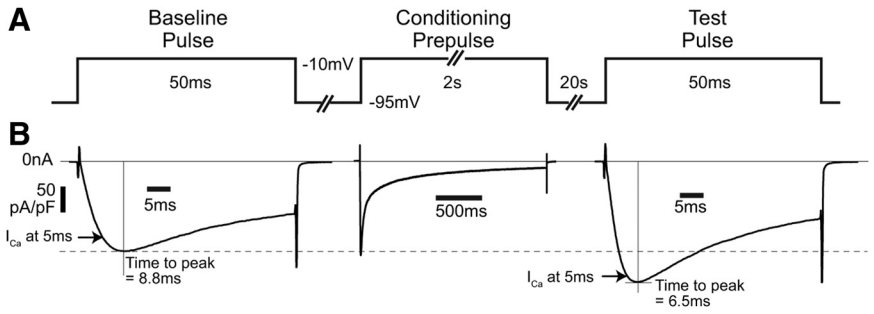

Figure 4. Evaluation of I_{Ca} activation kinetics after conditioning with a single test pulse. ***A***, Baseline and test voltage commands were prolonged to 50 ms to allow current to reach a maximum, and only a single test pulse was used to identify whether CDF requires multiple pulses as used in the basic protocol. ***B***, Current trace (typical of $n = 12$) shows that I_{Ca} 5 ms after initiating the test pulse is greater than the I_{Ca} at 5 ms in the baseline pulse (arrows), duplicating findings using the standard protocol. Additionally, the time to peak I_{Ca} (vertical lines) is shorter after the conditioning prepulse, and the peak I_{Ca} is greater after the conditioning prepulse compared with the baseline peak I_{Ca} (dashed line), indicating that increases in both the rate of I_{Ca} activation and the maximum I_{Ca} contribute to CDF as measured by 5 ms test pulses.

rometrically measured $R_{340/380}$ as an indicator $[Ca^{2+}]_c$ while simultaneously recording I_{Ca} recovery in the standard protocol (Fig. 5). Although this approach only detects global intracellular changes, the sensitivity of CDI and CDF to a slow Ca^{2+} chelator in the pipette (10 mM EGTA) suggests that global $[Ca^{2+}]_c$ may be more relevant for these processes than subplasmalemmal nanodomains. The transient increase in $[Ca^{2+}]_c$ triggered by conditioning depolarization resolved with a time constant of 2.2 ± 0.3 s ($n = 6$), resembling the pace of I_{Ca} recovery from initial inactivation (3.4 ± 1.5 s). Peak facilitation in these neurons (118 ± 4% of baseline) occurred at 17.3 ± 4.6 s after conditioning, by which time the depolarization-induced Ca^{2+} transient had fully resolved. Thus, CDI abates at approximately the same pace as the resolution of the Ca^{2+} transient, whereas CDF has either a delayed onset or a slower resolution than $[Ca^{2+}]_c$, and suggests that this form of I_{Ca} plasticity outlasts the Ca^{2+} transient.

CDF requires N-type channel function

To determine the source of Ca^{2+} responsible for CDI and CDF in sensory neurons, we first considered intracellular Ca^{2+} stores, since Ca^{2+} influx in sensory neurons triggers the process of Ca^{2+}-induced Ca^{2+} release (CICR) by which Ca^{2+} is discharged from intracellular stores through the ryanodine receptor channels (Gemes et al., 2009). This may add to the global increase in $[Ca^{2+}]_c$ and activate CaMKII (Shakiryanova et al., 2011). To disrupt CICR, sensory neurons were pretreated with the ryanodine receptor blocker dantrolene (10 μM), using conditions we have previously shown to limit Ca^{2+} release from intracellular stores in dissociated sensory neurons (Gemes et al., 2009). The lack of effect of dantrolene on %CDI or %CDF (Fig. 3*C*) suggests that Ca^{2+} released via CICR does not contribute to CDI and CDF.

Sensory neurons possess multiple subtypes of VGCCs, including L-, N-, P/Q-, and R- and T-type channels (Scroggs and Fox, 1992). To identify the specific VGCC subtypes involved in CDI and CDF, we used selective pharmacological blockers to isolate effects of L-type and N-type currents, since these convey the largest portions of total voltage-gated I_{Ca} in sensory neurons (Evans et al., 1996; Abdulla and Smith, 2001; McCallum et al., 2011). Blockade of N-type current by bath application of ω-conotoxin GVIA (200 nM) reduced peak I_{Ca} by ~50%, as expected (Fig. 6*A*). The effect on total Ca^{2+} influx during the conditioning prepulse (current integrated across time; Fig. 6*B*) was less, due to rapid current inactivation during the prepulse (Fig. 1*C*). Although CDI was not affected (Fig. 6*C*), the block of N-type current eliminated CDF (Fig. 6*D*). To determine whether reduced total I_{Ca} might itself contribute to diminished CDF regardless of

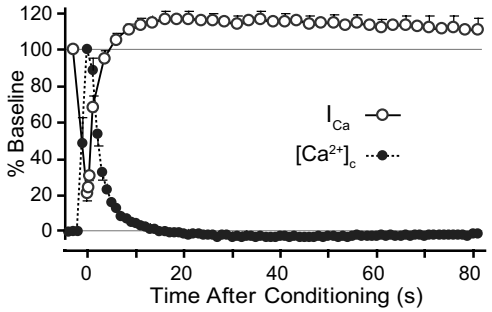

Figure 5. Time courses for I_{Ca} and cytoplasmic Ca^{2+} concentration ($[Ca^{2+}]_c$). I_{Ca} was measured during the standard protocol (Fig. 1*B*,*C*), and normalized to baseline. Fura-2 ratio of emission during excitation at 340 and 380 nm ($R_{340/380}$) was recorded simultaneously as an indicator of $[Ca^{2+}]_c$, which was normalized such that resting baseline is 0 and peak is 100. Averaged curves ($n = 6$) demonstrate that net inhibition of I_{Ca} is synchronous with $R_{340/380}$ elevation, but net facilitation of I_{Ca} outlasts return of $R_{340/380}$ to baseline.

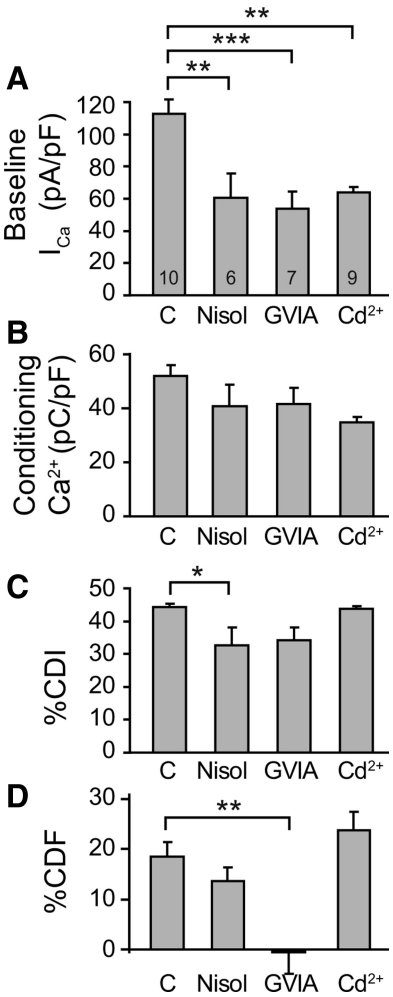

Figure 6. Effect of blockade of Ca^{2+} channel subtypes before, during, and after a conditioning prepulse. ***A–D***, Using the standard protocol, summary data are presented for the effect of VGCC blockers on (***A***) baseline I_{Ca} before the conditioning prepulse, (***B***) Ca^{2+} influx during the conditioning prepulse (i.e., I_{Ca} integrated over the 2 s depolarization), (***C***) CDI, measured as %CDI (Fig. 3*C*), and (***D***) CDF, measured as %CDF (Fig. 3*C*). Responses to the standard protocol were examined in matched groups of neurons treated with the L-type channel blocker nisoldipine (Nisol, 1 μM), with the N-type channel blocker ω-conotoxin GVIA (GVIA, 200 nM), the nonspecific Ca^{2+} channel blocker Cd^{2+} (3–6 μM), compared with untreated controls (C). Number of neurons for each group is shown in the bars. Brackets indicate significant differences. $^*p < 0.05$, $^{**}p < 0.01$, $^{***}p < 0.001$.

the path of entry, we titrated the nonselective VGCC blocker cadmium (3–6 μM) to produce a comparable overall reduction of I_{Ca} (Fig. 6*A*) and found that CDF was not diminished (Fig. 6*D*). Since cadmium will have partially reduced N-type I_{Ca}, this finding indicates that the dependence of CDF upon N-type current is not a simple proportionate relationship. L-type blockade using 1 μM nisoldipine ($K_d \sim 2$ nm) (Enyeart et al., 1986; Morel et al., 1998) also lowered total I_{Ca} to a similar extent (Fig. 6*A*). Although this reduced CDI by ~25% (Fig. 6*C*), it had no effect on CDF (Fig. 6*D*). Together, these observations indicate that CDF is not sensitive to total Ca^{2+} influx, but rather suggest a specific role for N-type Ca^{2+} channels as an effector site for generating sensory neuron CDF.

CDF is regulated by CaMKII

CDF has been shown to involve protein phosphorylation in other systems (see above), so we explored the potential regulation of N-type CDF in sensory neurons by two Ca^{2+}-sensitive kinases, CaMKII and protein kinase C (PKC) (Fig. 7*A–G*). The membrane-permeable CaMKII inhibitor KN-93 (2 μM) eliminated CDF, whereas the inactive analog KN-92 (2 μM) had no effect (Fig. 7*A*,*H*). KN-93 at this concentration additionally resulted in rundown of current in the absence of a conditioning prepulse (Fig. 7*A*), consistent with blockade of a potentiating effect of CaMKII on VGCCs. Alternatively, off-target direct effects of both KN-93 and KN-92 upon a variety of channels including VGCCs have been reported (Ledoux et al., 1999; Gao et al., 2006). These effects may also account for amplified inactivation during the prepulse, contributing to decreased Ca^{2+} influx (Fig. 7*F*) and apparent increased CDI (Fig. 7*G*), while elevated baseline I_{Ca} during KN-92 (Fig. 7*E*) is unexplained. Accordingly, we used a reduced KN-93 concentration (0.2 μM) to limit these off-target actions and found that this concentration of KN-93 eliminated facilitation (Fig. 7*B*,*H*) in the absence of other effects. In addition, CaMKII inhibition using a membrane-permeable peptide inhibitor of this kinase, mAIP (5 μM), also decreased facilitation, whereas myristoyl itself was inactive (Fig. 7*C*,*H*).

To test the effect of sustained blockade of CaMKII, we expressed AIP linked to GFP (GFP-AIP), using a construct that has been proved effective in inhibiting CaMKII (Bok et al., 2007). An AAV vector expressing either GFP-AIP or GFP alone was injected into L4 and L5 DRGs, from which neurons were dissociated 4 weeks later. Transduced neurons were identified for recording by GFP fluorescence, and had diameters (30.5 ± 1.9 μm, $n = 5$ for GFP-AIP; 29.3 ± 1.3 μm $n = 5$ for GFP; no difference between groups) comparable to other recorded neurons in this study. GFP-AIP eliminated CDF, while transduced neurons expressing only GFP produced typical CDF (Fig. 7*D*,*H*). Thus, for VGCCs in the sensory neuron system, pharmacological treatment of dissociated neurons as well as selective genetic manipulation in the intact animal reveal a dependence of CDF upon CaMKII activation.

Low-dose KN-93, mAIP, and GFP-AIP expression did not affect CDI (Fig. 7*G*), indicating that CaMKII selectively affects CDF but not CDI. PKC can enhance sensory neuron N-type and L-type I_{Ca} (Hall et al., 1995), but inhibition with chelerythrine (10 μM) did not affect baseline I_{Ca}, CDI, or CDF (Fig. 7*E–H*).

Injury eliminates CDF

We have previously found that peripheral nerve injury decreases CaMKII activity in sensory neurons (Kawano et al., 2009; Kojundzic et al., 2010). We therefore hypothesized that decreased CaMKII activity associated with neuronal injury should disrupt

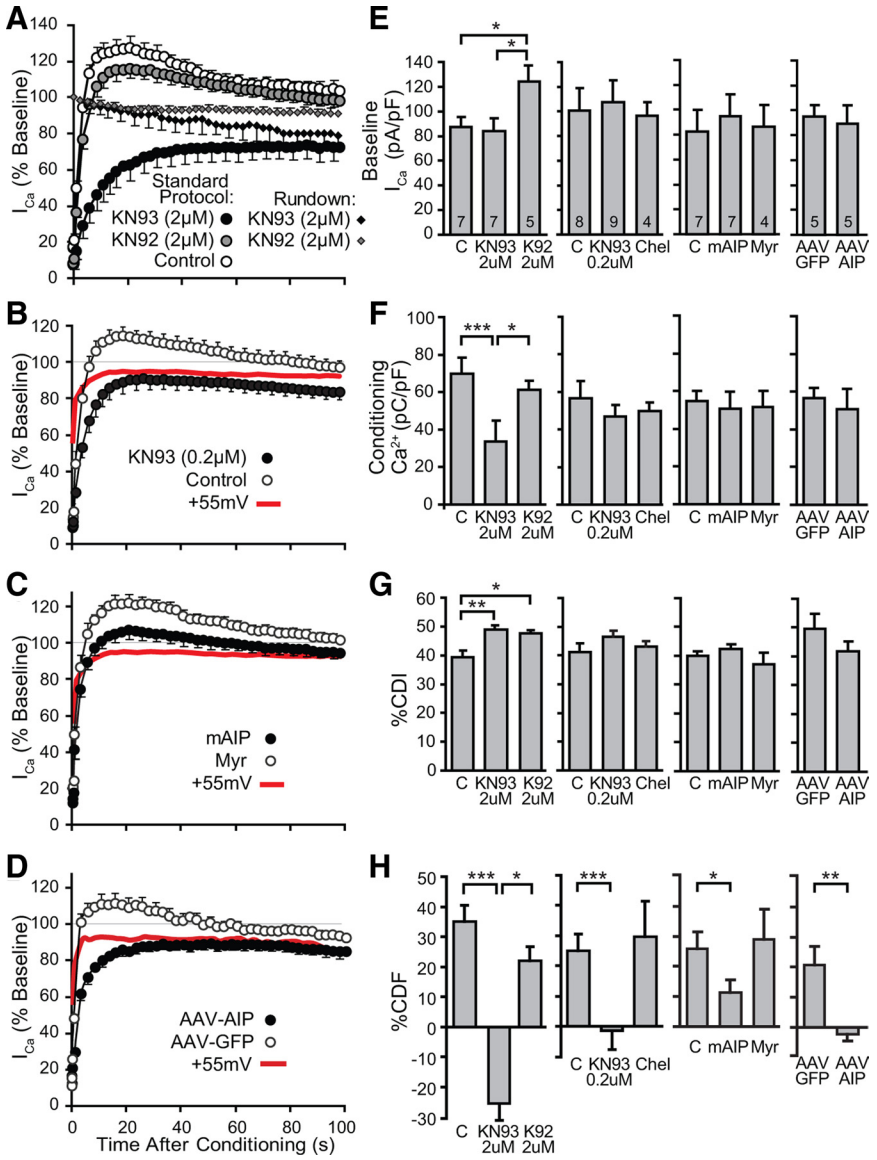

Figure 7. Effect of kinase inhibition on I_{Ca} before, during, and after a conditioning prepulse. ***A***, Using the standard protocol, the time course for recovery following a conditioning prepulse shows elimination of CDF by the CaMKII blocker KN-93 (2 μM, $n = 7$), but not by the inactive analog KN-92 (2 μM, $n = 5$), compared with matched control neurons ($n = 7$). In the absence of a conditioning prepulse, accelerated rundown is evident in neurons exposed to KN-93 (2 μM), suggesting a dependence of I_{Ca} upon CaMKII action. This rundown accounts for incomplete recovery after a conditioning prepulse in neurons exposed to KN-93. ***B***, A lower concentration of KN-93 (0.2 μM, $n = 8$) also suppresses CDF compared with matched controls ($n = 9$). The reference curve (+55 mV, red) is also shown. ***C***, The CaMKII inhibitory peptide mAIP (5 μM, $n = 7$) produces partial blockade of CDF compared with matched controls treated with myristoyl alone (Myr, 5 μM, $n = 7$). ***D***, Neurons harvested 4 weeks after *in vivo* transfection by AAV vectors show the effect of AIP linked to AIP (AAV-AIP, $n = 5$ neurons from 4 injected DRGs in 2 rats) or GFP expression alone (AAV-GFP, $n = 5$ neurons from 4 injected DRGs in 2 rats). Chronic CaMKII blockade by expressed AIP eliminated CDF. The reference curve (+55 mV, red) is derived from transduced neurons. ***E–H***, Summary data are presented for the effect of blockers on (***E***) baseline I_{Ca} before the conditioning prepulse, (***F***) Ca^{2+} influx during the conditioning prepulse (i.e., I_{Ca} integrated over the 2 s depolarization), (***G***) CDI, measured as %CDI (Fig. 3*B*), and (***H***) CDF, measured as %CDF (Fig. 3*B*). The PKC inhibitor chelerythrine (Chel, 10 μM) and myristoyl (Myr, 5 μM) had no effects. Separate untreated control groups (C) are shown with their matched treated groups. Negative calculated values of %CDF for neurons treated with KN-93 represent failure of I_{Ca} to recover to matched recordings using prepulse depolarization to +55 mV (data not shown). Number of neurons for each group is shown in the bars. Brackets indicate significant differences. $^*p < 0.05$, $^{**}p < 0.01$, $^{***}p < 0.001$.

CDF generation. Nerve injury by SNL results in axotomy of the L5 DRG neurons, while the neighboring L4 neurons are exposed to inflammation initiated by the degenerating distal L5 axon segments. Since the relative contributions of these two populations to pain behavior have not been established (Gold, 2000), we examined Ca^{2+}-dependent regulation of I_{Ca} in neurons from both ganglia separately. Recordings were performed 21–30 d after injury since this allows nonspecific effects of surgery to subside and reflects the chronic phase of neuropathy. At that time, behavioral testing of the rats injured by SNL demonstrated hyperalgesia (39 ± 3% hyperalgesia-type response to pin touch, $n = 37$) in contrast to animals receiving only skin incision (0 ± 0%, $n = 101$; $p < 0.001$). Comparison of neurons from SNL and skin incision animals revealed distinct effects of injury on I_{Ca} and its regulation by neuronal activity (Fig. 8*A*,*B*). Consistent with our previous findings (McCallum et al., 2006), baseline I_{Ca} (Fig. 8*C*) as well as Ca^{2+} influx during the conditioning prepulse (Fig. 8*D*) were decreased in L5 neurons after SNL, compared with matched neurons from control rats. The extent of CDI was unaffected by SNL in both the L4 and L5 neurons (Fig. 8*E*). However, there was an almost complete loss of CDF after axotomy of the directly injured L5 neurons, and a less complete loss of CDF in the L4 neurons indirectly affected by SNL (Fig. 8*F*). We considered the possibility that the injury-induced reduction of Ca^{2+} influx during the prepulse was responsible for the disappearance of CDF, and tested this by increasing influx in SNL L5 neurons. Because of I_{Ca} inactivation, prolongation of the prepulse to 4 s minimally increased total influx (7.5 ± 2.5%, $n = 5$). Raising bath Ca^{2+} to 4 mM, however, successfully elevated influx (Fig. 8*D*), but this did not rescue CDF in the axotomized SNL L5 neurons (Fig. 8*E*). Additionally, in control neurons, there was no influence of Ca^{2+} influx upon %CDF (linear regression $R^2 = 0.02$, $p = 0.35$). These findings show not only that CDI and CDF have distinct mechanistic pathways but also that injury disrupts the natural regulation of I_{Ca}.

Physiological role of CDF in sensory neurons

To place sensory neuron CDF into a natural context, we examined whether conditioning stimuli would produce CDF under conditions that duplicate a physiological setting. We first examined conditioning from a holding potential of −65 mV to replicate the resting membrane potential of sensory neurons (Sapunar et al., 2005). Under these conditions, %CDF (normalized by comparison to a reference curve using a depolarization step to +55 mV from a holding potential of −65 mV) was 19 ± 6% (Fig. 9*A*; $n = 9$). This confirms that CDF in sensory neurons evolves after neuronal activity even with a physiological resting membrane potential. We next examined the nature of the conditioning stimulus. Since depolarizations in the form of a pulse train accentuate cumulative VDI compared with sustained (square wave) depolar-

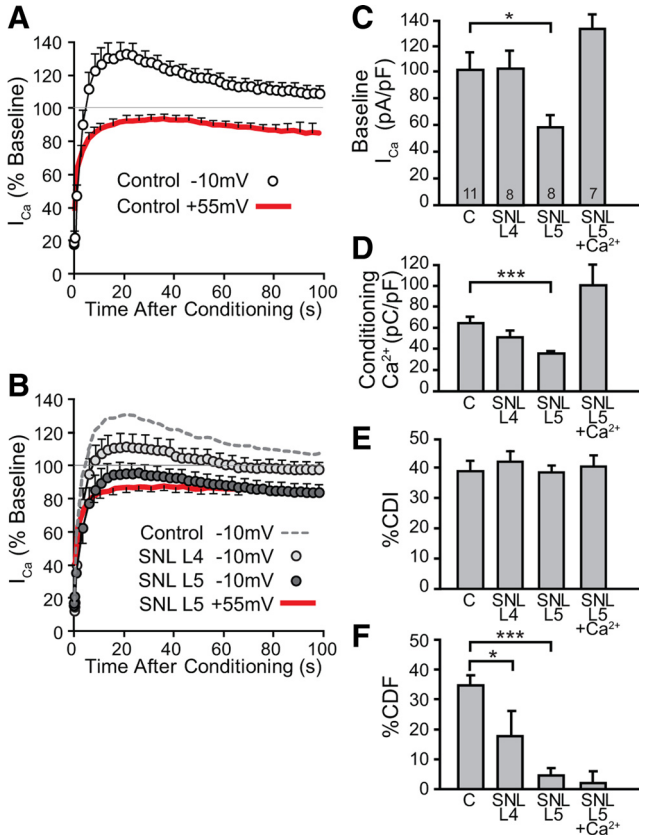

Figure 8. Effect of painful nerve injury on I_{Ca} before, during, and after a conditioning prepulse. ***A***, In uninjured control neurons, the time course for I_{Ca} recovery was evaluated after a conditioning prepulse to either −10 mV or +55 mV ($n = 12$ for each). ***B***, Matched observations made in neurons dissociated from animals subjected to SNL showed marked suppression of CDF in the axotomized neurons from the fifth lumbar level (SNL L5, $n = 8$) and partial suppression in the neighboring neurons (SNL L4, $n = 8$), compared with uninjured control neurons (dashed line, same data as in ***A***). Prepulse depolarizations to +55 mV were recorded for SNL L5 (red, $n = 8$) and SNL L4 (data not shown, $n = 8$). ***C–F***, Summary data are presented for the effect of injury on (***C***) baseline I_{Ca} before the conditioning prepulse, (***D***) Ca^{2+} influx during the conditioning prepulse (i.e., I_{Ca} integrated over the 2 s depolarization), (***E***) CDI, measured as ΔR_{CDI} (Fig. 3*C*), and (***F***) CDF, measured as ΔR_{CDF} (Fig. 3*C*). SNL L5 neurons show decreased baseline I_{Ca}, decreased Ca^{2+} influx during the conditioning prepulse, and substantial decrease of CDF compared with control neurons. Elevation of bath Ca^{2+} to 4 mM (SNL L5 + Ca^{2+}) increased Ca^{2+} influx in SNL L5 neurons to above normal levels, but this did not rescue CDF. Number of neurons for each group is shown in the bars. Brackets indicate significant differences. $^{*}p < 0.05$, $^{***}p < 0.001$.

ization (Patil et al., 1998), it is possible that CDF during recovery from neuronal activation might be seen only after nonpulsatile depolarization. To test this, we used a conditioning stimulus in the pattern of an AP train (Fig. 9*B*), replicating natural neuronal activity. CDF was again observed after this form of neuronal activation (facilitation to a maximum of 117% in each of two neurons). These observations indicate that CDF occurs under physiological conditions in sensory neurons.

Cytoplasmic Ca^{2+} critically controls repetitive firing behavior in sensory neurons. Specifically, Ca^{2+} that enters through VGCCs opens Ca^{2+}-sensitive K^{+} channels that are expressed by peripheral sensory neurons (Sarantopoulos et al., 2007), thereby inhibiting repetitive AP firing (Hogan et al., 2008; Lirk et al., 2008). We therefore directly examined whether CDI and CDF triggered by neuronal depolarization influence the subsequent generation of APs in repetitively firing small- to medium-sized sensory neurons (diameter 31 ± 1 μm; input resistance 73 ± 7 MΩ; resting membrane potential −58 ± 1 mV; no differences between the conditioned group, $n = 52$, and the time control group, $n = 22$). Recordings were performed by an intracellular technique to minimize disturbance of cytoplasmic Ca^{2+} signaling (Friel and Tsien, 1992) and in intact DRGs to eliminate the effects of dissociation. At various intervals following a conditioning prepulse (0 mV, 2 s, voltage-clamp), we determined the number of APs during a test pulse (2 nA, 50 ms, current-clamp), which was compared with the number of APs generated by an identical baseline pulse 15 s before conditioning (Fig. 10*A*). Control recordings were made in other neurons from the same ganglion, using the same protocol but without the conditioning prepulse (Fig. 10*B*). The number of APs produced by current injection was unchanged at 0.5, 1, and 2 s following the conditioning prepulse (Fig. 10*C*), indicating that repetitive firing was not affected during the initial period following the conditioning prepulse. However, AP generation decreased with longer intervals and was reduced to approximately half of baseline at 10 s following the conditioning prepulse, with subsequent recovery thereafter. This time course was comparable to that for the development of CDF following a conditioning prepulse in dissociated neurons. To confirm that regulation of excitability is attributable to the operation of CDF, we examined the Ca^{2+} dependence of this process using a similar protocol in dissociated sensory neurons delivered by whole-cell patch technique (Fig. 11*A*). Whereas excitability was suppressed by the conditioning prepulse in control neurons with standard pipette solution (0.5 mM EGTA; Fig. 11*B*), this effect was lost when Ca^{2+} influx was buffered with high pipette EGTA (10 mM; Fig. 11*C*). These findings suggest that under natural conditions, CDF functions as a potent throttle that suppresses sensory neuron excitability following a period of intense neuronal activity.

Since our observations in dissociated neurons indicate a loss of CDF after neuronal injury, we speculated that this would compromise the control of excitability after a conditioning prepulse. At the time point (10 s) at which control neurons showed maximal suppression of repetitive firing following a conditioning prepulse, neurons subjected to SNL (diameter 32 ± 1 μm; input resistance 72 ± 8 MΩ; resting membrane potential −58 ± 2 mV; no differences between the conditioned group, $n = 13$, and the time control group, $n = 11$) showed no effect of the conditioning prepulse on AP generation (Fig. 10*D*). This indicates that the CDF mechanism for regulating excitability after intense neuronal activation is lost following axonal injury of sensory neurons.

Sensory neurons are exposed to repeated volleys of APs, and it is possible that the presence of CDF modulates processes underlying inactivation (VDI and CDI). We evaluated this by applying a second conditioning pulse after establishing CDF by a previous conditioning pulse in control neurons (Fig. 12). Total inactivation was independent of pre-existing CDF, and CDF was fully re-established after recovery from inactivation. Axotomized SNL L5 neurons ($n = 3$) similarly showed a response to a second conditioning pulse that was comparable to the first (data not shown).

Discussion

The central role of Ca^{2+} in coordinating neuronal function suggests dysregulation of Ca^{2+} signaling as a potential cause of neuropathic pain. We have identified robust Ca^{2+}-dependent modulation of I_{Ca} in DRG neurons that is distinct from VDI. Unlike CDI, CDF is regulated by CaMKII and is lost following neuronal injury, a process that increases neuronal excitability and may contribute to neuropathic pain.

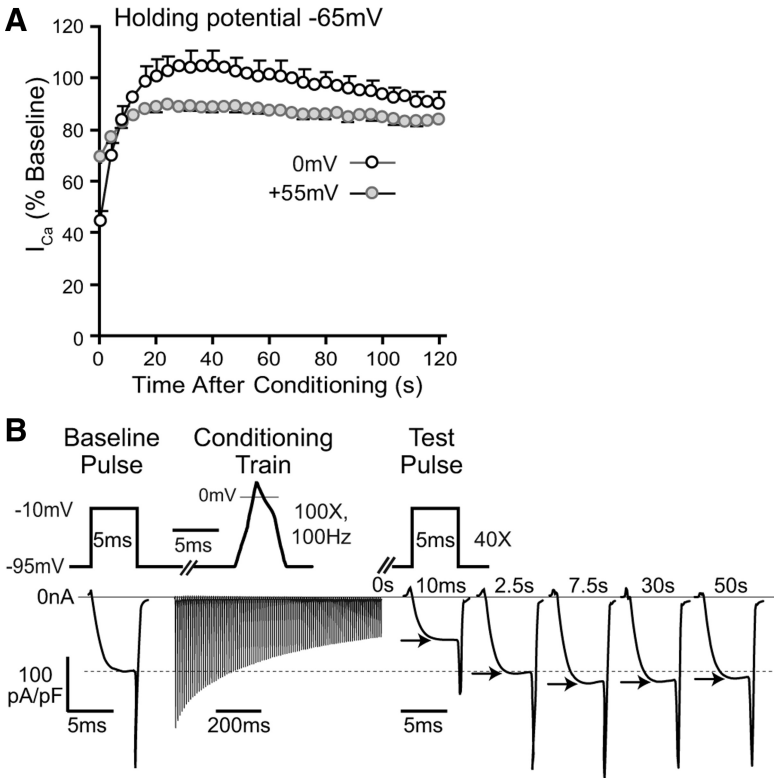

Figure 9. Influence of depolarization from a holding potential of −65 mV and conditioning by an impulse train. ***A***, When a holding potential of −65 mV is used, a depolarizing conditioning prepulse (0 mV, 2 s; $n = 9$) is followed by facilitation, whereas a prepulse to +55 mV does not produce facilitation ($n = 8$). This protocol used test pulses starting at 10 ms after the prepulse and then at 2.5 s intervals. ***B***, Facilitation also followed a conditioning stimulus composed of a train of AP waveform commands (100 APs at 100 Hz), as represented by the I_{Ca} that exceeded baseline when evoked by a test pulse 7.5 s after conditioning.

CDI in sensory neurons

A contribution of CDI to I_{Ca} inactivation during sustained depolarization has been shown in previous investigations of N-type and P/Q-type currents in neurons (Cox and Dunlap, 1994; Chaudhuri et al., 2005) and in expressed L-, N-, R-, and P/Q-type channels (Lee et al., 1999; Liang et al., 2003), where its extent is modulated by coexpression of particular auxiliary β-subunits (Lee et al., 2000). We observed I_{Ca} inactivation that is synchronous with the maximal $[Ca^{2+}]_c$ and is sensitive to cytoplasmic Ca^{2+} buffering, consistent with prior observations in a variety of expressed VGCC subtypes, for which CaM-dependent CDI is responsive to global cytoplasmic Ca^{2+} accumulation (Lee et al., 1999; Liang et al., 2003; Chaudhuri et al., 2007). CDI at sensory neuron central terminals may contribute to short-term synaptic depression as has been noted for P/Q-type currents in the calyx of Held (Forsythe et al., 1998; Xu and Wu, 2005), thereby enhancing the temporal contrast for sensations conveyed by high intensity afferent activity.

CDF in sensory neurons

While CDF has been observed for P/Q channels in the CNS (Borst and Sakmann, 1998; Chaudhuri et al., 2005), its presence in peripheral sensory neurons or the participation of other neuronal VGCC subtypes in CDF have not previously been reported. It is unlikely that our observations represent voltage-dependent facilitation (Kavalali and Plummer, 1994) or relief of tonic G-protein-mediated inhibition (Ikeda, 1991; Zamponi and Snutch, 1998) since depolarization to +55 mV did not produce facilitation, and sensitivity to PKC that typifies G-protein-mediated inhibition was absent (Swartz, 1993). Several lines of evidence support a direct role of Ca^{2+} in producing I_{Ca} facilitation. First, depolarization to a potential that admitted minimal Ca^{2+} eliminated facilitation. Second, replacement of extracellular Ca^{2+} with Ba^{2+} similarly reduced facilitation, which indicates a specific dependence on Ca^{2+} as the permeant cation. Third, we observed that CDF of N-type currents is sensitive to high cytoplasmic Ca^{2+} buffering, indicating that globally increased cytoplasmic Ca^{2+} is necessary to initiate CDF in sensory neurons. This contrasts with CDF in cerebellar P-type channels, which is dependent on Ca^{2+} elevation only in the nanodomain around individual channels (Chaudhuri et al., 2005), but concurs with findings from brainstem and expressed P/Q channels and myocyte L-type channels (Xiao et al., 1994; Borst and Sakmann, 1998; Lee et al., 2000).

In our observations of sensory neurons, persistence of CDF beyond the period of elevated $[Ca^{2+}]_c$ suggests involvement of factors other than a simple action on CaM. This sustained effect is compatible with the participation of CaMKII, which retains activity through autophosphorylation even after CaM dissociates (Saitoh and Schwartz, 1985). A role for CaMKII is further suggested by the sensitivity of CDF to Ca^{2+} buffering, and by the efficacy of CaMKII blockers in limiting CDF. Together, these observations indicate that CaMKII is a central component of a signaling cascade triggered by neuronal activity that ultimately activates Cav2.2 channels. While we could not discern the onset kinetics of CDF in our model due to concurrent VDI and CDI, slow activation of CaMKII may account for the delayed peak of CDF, as has been noted for the CaMKII-dependent facilitation of L-type I_{Ca} in cardiac myocytes after photorelease of Ca^{2+} (Anderson et al., 1994). Alternatively, CDF may activate rapidly but is obscured by CDI. Brain N-type Ca^{2+} channels are recognized targets of CaMKII and PKC phosphorylation (Hell et al., 1994), although our data do not reveal participation of PKC in generating CDF. Resolving the specific downstream effects of CaMKII leading to sensory neuron CDF, for instance phosphorylation of the Synprint region of α1-subunits (Yokoyama et al., 1997, 2005) or prolongation of channel open probability (Dzhura et al., 2000), awaits future studies.

The dominant path for activity-induced Ca^{2+} influx in small- to medium-sized sensory neurons is through L-type and N-type VGCCs (Evans et al., 1996; Abdulla and Smith, 2001; McCallum et al., 2011). In our present experiments, blockade of N-type VGCCs eliminated CDF, which suggests either that Ca^{2+} entering through N-type channels may be uniquely able to activate CaMKII, or that CaMKII selectively enhances N-type Ca^{2+} channel function in sensory neurons under these conditions. The first scenario seems unlikely since this model favors localized coupling between the N-type calcium channel and CaMKII, which is not supported by elimination of CDF with high cytoplasmic Ca^{2+} buffering. The alternative possibility that CaMKII produces CDF

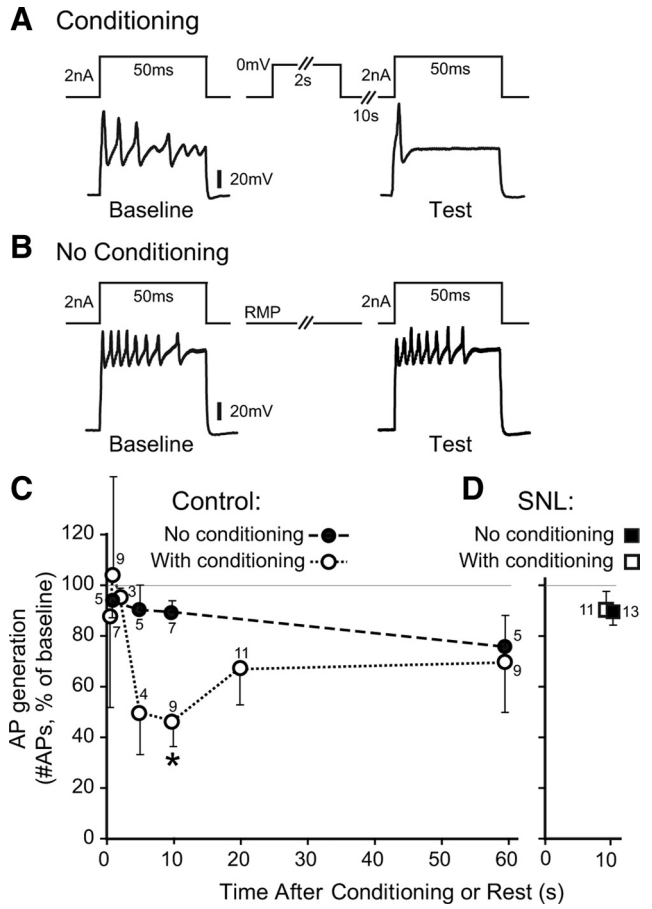

Figure 10. Effect of a conditioning prepulse on excitability of nondissociated sensory neurons recorded by intracellular microelectrode. ***A***, AP firing induced by depolarizing current test pulses was diminished 10 s after a conditioning prepulse in a control neuron (28 μm diameter) from an uninjured L5 DRG. ***B***, In the absence of conditioning, a different control neuron (38 μm) showed no change in AP generation after a comparable interval. ***C***, The time course for excitability (the ratio of APs generated during the test pulse normalized to baseline) is shown for test pulses applied at various time intervals after conditioning. Only a single test pulse was applied to each neuron. Control neurons (L5 DRG) show depression of excitability 10 s after conditioning compared with neurons without conditioning. ***D***, After injury by L5 SNL, the conditioning prepulse failed to suppress excitability in axotomized L5 neurons. Note that both of the SNL data points (with and without conditioning prepulse) are at 10 s, but are displayed slightly offset for clarity. Mean ± SEM, numbers next to data points indicate *n* for neurons. $*p < 0.05$.

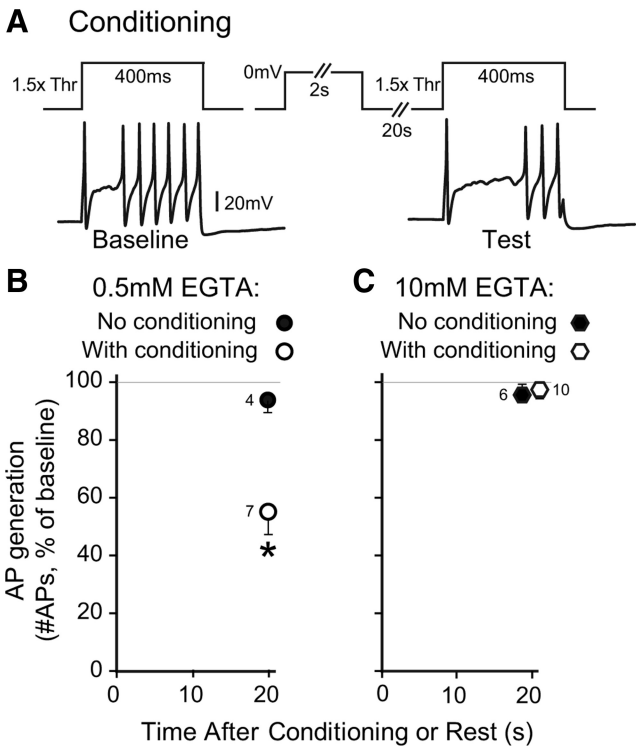

Figure 11. Effect of a conditioning prepulse on excitability of dissociated sensory neurons recorded by patch technique. ***A***, Similar to the recordings in nondissociated neurons shown in Figure 10, AP firing induced by depolarizing current test pulses was diminished 20 s after a conditioning prepulse in a control neuron (25 μm diameter) recorded with standard pipette solution (0.5 mM EGTA). Whereas conditioning decreases excitability (the ratio of APs generated during the test pulse normalized to baseline) with standard pipette buffering (***B***), high buffering (10 mM EGTA) eliminates the effect of conditioning on excitability (***C***). Note that both of the data points for 10 mM EGTA (with and without conditioning prepulse) are at 20 s, but are displayed slightly offset for clarity. Mean ± SEM, numbers next to data points indicate *n* for neurons. $*p < 0.05$.

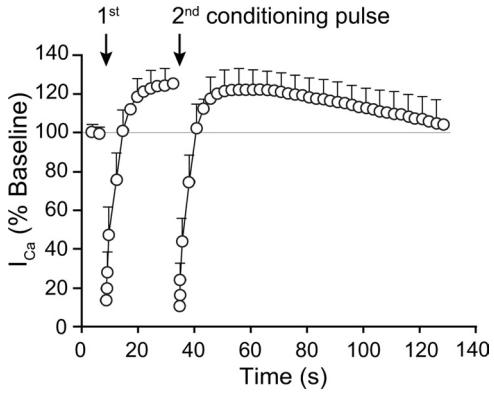

Figure 12. Influence of pre-existing CDF on the response of I_{Ca} to neuronal activation. The development of both I_{Ca} inactivation and facilitation in control neurons ($n = 5$) are unchanged in response to a second conditioning pulse delivered during preexisting CDF, compared with the response to the initial conditioning pulse. Mean ± SEM.

in N-type calcium channels is particularly intriguing, as this form of plasticity has never been reported in neurons.

Influence of injury

Only minimal CDF remains in neurons injured by peripheral axotomy. This cannot be attributed to exaggerated inactivation by CDI and VDI, as these were unchanged by injury, so some component of the mechanistic sequence that generates CDF must become deficient after injury. Previous findings show that axotomy reduces I_{Ca} N-type current, but this is only an incomplete effect (<50%) (Baccei and Kocsis, 2000; Abdulla and Smith, 2001; McCallum et al., 2011). An additional likely factor is impaired CaMKII signaling following nerve injury, which we have found to occur selectively in animals that develop pain behavior (Kawano et al., 2009; Kojundzic et al., 2010). Although our present experiments focused on I_{Ca} responses to phasic $[Ca^{2+}]_c$ changes evoked by neuronal activation, the failure of GFP-AIP expression to lower baseline I_{Ca} indicates that tonically lowered CaMKII activity is not likely to account for depressed baseline I_{Ca} after injury.

Potential consequences of CDF in sensory neurons: divergent physiological effects at different cellular sites

Our data indicate that Ca^{2+} signaling via CaMKII enhances VGCC function in the sensory neuron soma after intense neuro-

nal stimulation. Although confirmation that a similar phenomenon occurs in neurites and synaptic terminals awaits further study, we can consider what physiological effects may be expected. CaMKII is known to be present in presynaptic terminals in other tissues such as hippocampus (Nayak et al., 1996), and N-type Ca^{2+} channels are the dominant presynaptic Ca^{2+} influx pathway for synaptic transmission of nociceptive activity in the spinal dorsal horn (Matthews and Dickenson, 2001; Heinke et al., 2004; Rycroft et al., 2007). If these elements interact in the sensory neuron central terminals as we have observed in the soma, CDF may be a key process in pain signaling. Since neurotransmitter release is proportional to the third or fourth power of Ca^{2+} entry (Dodge and Rahamimoff, 1967; Sakaba and Neher, 2001), CDF would be a powerful mechanism for amplifying presynaptic function. For instance, by increasing I_{Ca} 34%, the CDF that we observed would elevate neurotransmitter release threefold. This would enhance synaptic transmission after intense sensory stimulation, resulting in sensory sensitization during the time period of CDF action. Activity-induced enhanced synaptic transmission in dorsal horn pain pathways is thought to be a critical feature contributing to some chronic pain states (Latremoliere and Woolf, 2009).

Since Ca^{2+} regulates numerous cellular processes, the net influence of CDF on sensory neuron excitability is hard to predict and may differ in various subgroups and in different parts of the neuron. In the specific setting of peripheral nerve trauma, our finding that CDF is lost suggests that the dominant site of CDF action may not be the synaptic terminal. In the peripheral nervous system, our data show decreased AP generation in sensory neuron somata following a conditioning stimulus that induces CDF. Thus, CDF appears to provide a negative feedback upon membrane excitability after a period of intense activity. This is explainable by the rapid activation of dominant K^+ currents by Ca^{2+} influx (Raman and Bean, 1999), producing a net outward current and decreased membrane resistance that suppress repetitive firing (Scholz et al., 1998; Swensen and Bean, 2003; Lirk et al., 2008). Similar CDF in the peripheral termini of sensory neurons would contribute to sensory adaptation, since a stimulus-induced pulse train would be followed by a period in which CDF produces relative suppression of repetitive AP generation. CDF in the membrane of the sensory neuron T-junction would be expected to intensify the Ca^{2+}-regulated filtering of afferent AP trains, which would also diminish the amount of sensory traffic reaching the spinal dorsal horn following intense afferent activity (Stoney, 1990; Lüscher et al., 1994, 1996). The overall resulting effect of CDF acting at peripheral sites could therefore be sensory desensitization following intense activation, for instance the temporary relief from itch provided by intense counterstimuli (Ward et al., 1996).

At the sensory neuron soma, initiation of APs occurs only under pathological conditions, including peripheral nerve injury (Devor, 2006). Our present findings indicate that CDF at this site is lost after peripheral axotomy, which could further amplify ectopic activity originating in DRG somata due to loss of the braking action that CDF applies to repetitive AP generation. This can be expected to result in longer and more frequent bursts of activity, and therefore could be an important element contributing to spontaneous pain and paresthesias following peripheral nerve injury.

References

Abdulla FA, Smith PA (2001) Axotomy- and autotomy-induced changes in Ca2+ and K+ channel currents of rat dorsal root ganglion neurons. J Neurophysiol 85:644–658.

Anderson ME, Braun AP, Schulman H, Premack BA (1994) Multifunctional Ca2+/calmodulin-dependent protein kinase mediates Ca(2+)-induced enhancement of the L-type Ca2+ current in rabbit ventricular myocytes. Circ Res 75:854–861.

Anderson ME, Braun AP, Wu Y, Lu T, Schulman H, Sung RJ (1998) KN-93, an inhibitor of multifunctional Ca++/calmodulin-dependent protein kinase, decreases early afterdepolarizations in rabbit heart. J Pharmacol Exp Ther 287:996–1006.

Baccei ML, Kocsis JD (2000) Voltage-gated calcium currents in axotomized adult rat cutaneous afferent neurons. J Neurophysiol 83:2227–2238.

Berridge MJ, Lipp P, Bootman MD (2000) The versatility and universality of calcium signalling. Nat Rev Mol Cell Biol 1:11–21.

Blaich A, Welling A, Fischer S, Wegener JW, Köstner K, Hofmann F, Moosmang S (2010) Facilitation of murine cardiac L-type Ca(v)1.2 channel is modulated by calmodulin kinase II-dependent phosphorylation of S1512 and S1570. Proc Natl Acad Sci U S A 107:10285–10289.

Bok J, Wang Q, Huang J, Green SH (2007) CaMKII and CaMKIV mediate distinct prosurvival signaling pathways in response to depolarization in neurons. Mol Cell Neurosci 36:13–26.

Borst JG, Sakmann B (1998) Facilitation of presynaptic calcium currents in the rat brainstem. J Physiol 513:149–155.

Chaudhuri D, Alseikhan BA, Chang SY, Soong TW, Yue DT (2005) Developmental activation of calmodulin-dependent facilitation of cerebellar P-type Ca2+ current. J Neurosci 25:8282–8294.

Chaudhuri D, Issa JB, Yue DT (2007) Elementary mechanisms producing facilitation of Cav2.1 (P/Q-type) channels. J Gen Physiol 129:385–401.

Cox DH, Dunlap K (1994) Inactivation of N-type calcium current in chick sensory neurons: calcium and voltage dependence. J Gen Physiol 104:311–336.

Cuttle MF, Tsujimoto T, Forsythe ID, Takahashi T (1998) Facilitation of the presynaptic calcium current at an auditory synapse in rat brainstem. J Physiol 512:723–729.

DeMaria CD, Soong TW, Alseikhan BA, Alvania RS, Yue DT (2001) Calmodulin bifurcates the local Ca2+ signal that modulates P/Q-type Ca2+ channels. Nature 411:484–489.

Devor M (2006) Response of nerves to injury in relation to neuropathic pain. In: Wall and Melzack's textbook of pain, Ed 5 (McMahon S, Koltzenburg M, eds), pp 905–927. London: Churchill Livingstone.

Dodge FA Jr, Rahamimoff R (1967) Co-operative action a calcium ions in transmitter release at the neuromuscular junction. J Physiol 193:419–432.

Dzhura I, Wu Y, Colbran RJ, Balser JR, Anderson ME (2000) Calmodulin kinase determines calcium-dependent facilitation of L-type calcium channels. Nat Cell Biol 2:173–177.

Enyeart JJ, Aizawa T, Hinkle PM (1986) Interaction of dihydropyridine Ca2+ agonist Bay K 8644 with normal and transformed pituitary cells. Am J Physiol 250:C95–102.

Evans AR, Nicol GD, Vasko MR (1996) Differential regulation of evoked peptide release by voltage-sensitive calcium channels in rat sensory neurons. Brain Res 712:265–273.

Fischer G, Kostic S, Nakai H, Park F, Sapunar D, Yu H, Hogan Q (2011) Direct injection into the dorsal root ganglion: technical, behavioral, and histological observations. J Neurosci Methods 199:43–55.

Forsythe ID, Tsujimoto T, Barnes-Davies M, Cuttle MF, Takahashi T (1998) Inactivation of presynaptic calcium current contributes to synaptic depression at a fast central synapse. Neuron 20:797–807.

Friel DD, Tsien RW (1992) A caffeine- and ryanodine-sensitive Ca2+ store in bullfrog sympathetic neurones modulates effects of Ca2+ entry on [Ca2+]i. J Physiol 450:217–246.

Fuchs A, Rigaud M, Hogan QH (2007a) Painful nerve injury shortens the intracellular Ca2+ signal in axotomized sensory neurons of rats. Anesthesiology 107:106–116.

Fuchs A, Rigaud M, Sarantopoulos CD, Filip P, Hogan QH (2007b) Contribution of calcium channel subtypes to the intracellular calcium signal in sensory neurons: the effect of injury. Anesthesiology 107:117–127.

Gao L, Blair LA, Marshall J (2006) CaMKII-independent effects of KN93 and its inactive analog KN92: reversible inhibition of L-type calcium channels. Biochem Biophys Res Commun 345:1606–1610.

Gemes G, Rigaud M, Weyker PD, Abram SE, Weihrauch D, Poroli M, Zoga V, Hogan QH (2009) Depletion of calcium stores in injured sensory neurons: anatomic and functional correlates. Anesthesiology 111:393–405.

Gemes G, Rigaud M, Koopmeiners AS, Poroli MJ, Zoga V, Hogan QH (2010) Calcium signaling in intact dorsal root ganglia: new observations and the effect of injury. Anesthesiology 113:134–146.

Gold MS (2000) Spinal nerve ligation: what to blame for the pain and why. Pain 84:117–120.

Grimm D, Zhou S, Nakai H, Thomas CE, Storm TA, Fuess S, Matsushita T, Allen J, Surosky R, Lochrie M, Meuse L, McClelland A, Colosi P, Kay MA (2003) Preclinical in vivo evaluation of pseudotyped adeno-associated virus vectors for liver gene therapy. Blood 102:2412–2419.

Grueter CE, Abiria SA, Dzhura I, Wu Y, Ham AJ, Mohler PJ, Anderson ME, Colbran RJ (2006) L-type Ca2+ channel facilitation mediated by phosphorylation of the beta subunit by CaMKII. Mol Cell 23:641–650.

Hadley RW, Lederer WJ (1991) Ca2+ and voltage inactivate Ca2+ channels in guinea-pig ventricular myocytes through independent mechanisms. J Physiol 444:257–268.

Hall KE, Browning MD, Dudek EM, Macdonald RL (1995) Enhancement of high threshold calcium currents in rat primary afferent neurons by constitutively active protein kinase C. J Neurosci 15:6069–6076.

Heinke B, Balzer E, Sandkühler J (2004) Pre- and postsynaptic contributions of voltage-dependent Ca2+ channels to nociceptive transmission in rat spinal lamina I neurons. Eur J Neurosci 19:103–111.

Hell JW, Appleyard SM, Yokoyama CT, Warner C, Catterall WA (1994) Differential phosphorylation of two size forms of the N-type calcium channel alpha 1 subunit which have different COOH termini. J Biol Chem 269:7390–7396.

Hogan QH, McCallum JB, Sarantopoulos C, Aason M, Mynlieff M, Kwok WM, Bosnjak ZJ (2000) Painful neuropathy decreases membrane calcium current in mammalian primary afferent neurons. Pain 86:43–53.

Hogan Q, Sapunar D, Modric-Jednacak K, McCallum JB (2004) Detection of neuropathic pain in a rat model of peripheral nerve injury. Anesthesiology 101:476–487.

Hogan Q, Lirk P, Poroli M, Rigaud M, Fuchs A, Fillip P, Ljubkovic M, Gemes G, Sapunar D (2008) Restoration of calcium influx corrects membrane hyperexcitability in injured rat dorsal root ganglion neurons. Anesth Analg 107:1045–1051.

Hudmon A, Schulman H, Kim J, Maltez JM, Tsien RW, Pitt GS (2005) CaMKII tethers to L-type Ca2+ channels, establishing a local and dedicated integrator of Ca2+ signals for facilitation. J Cell Biol 171:537–547.

Ikeda SR (1991) Double-pulse calcium channel current facilitation in adult rat sympathetic neurones. J Physiol 439:181–214.

Jiang X, Lautermilch NJ, Watari H, Westenbroek RE, Scheuer T, Catterall WA (2008) Modulation of CaV2.1 channels by Ca2+/calmodulin-dependent protein kinase II bound to the C-terminal domain. Proc Natl Acad Sci U S A 105:341–346.

Kavalali ET, Plummer MR (1994) Selective potentiation of a novel calcium channel in rat hippocampal neurones. J Physiol 480:475–484.

Kawano T, Zoga V, Gemes G, McCallum JB, Wu HE, Pravdic D, Liang MY, Kwok WM, Hogan Q, Sarantopoulos C (2009) Suppressed Ca2+/CaM/CaMKII-dependent K(ATP) channel activity in primary afferent neurons mediates hyperalgesia after axotomy. Proc Natl Acad Sci U S A 106:8725–8730.

Kim SH, Chung JM (1992) An experimental model for peripheral neuropathy produced by segmental spinal nerve ligation in the rat. Pain 50:355–363.

Kojundzic SL, Puljak L, Hogan Q, Sapunar D (2010) Depression of Ca(2+)/calmodulin-dependent protein kinase II in dorsal root ganglion neurons after spinal nerve ligation. J Comp Neurol 518:64–74.

Latremoliere A, Woolf CJ (2009) Central sensitization: a generator of pain hypersensitivity by central neural plasticity. J Pain 10:895–926.

Ledoux J, Chartier D, Leblanc N (1999) Inhibitors of calmodulin-dependent protein kinase are nonspecific blockers of voltage-dependent K+ channels in vascular myocytes. J Pharmacol Exp Ther 290:1165–1174.

Lee A, Wong ST, Gallagher D, Li B, Storm DR, Scheuer T, Catterall WA (1999) Ca2+/calmodulin binds to and modulates P/Q-type calcium channels. Nature 399:155–159.

Lee A, Scheuer T, Catterall WA (2000) Ca2+/calmodulin-dependent facilitation and inactivation of P/Q-type Ca2+ channels. J Neurosci 20:6830–6838.

Lee SJ, Escobedo-Lozoya Y, Szatmari EM, Yasuda R (2009) Activation of CaMKII in single dendritic spines during long-term potentiation. Nature 458:299–304.

Liang H, DeMaria CD, Erickson MG, Mori MX, Alseikhan BA, Yue DT (2003) Unified mechanisms of Ca2+ regulation across the Ca2+ channel family. Neuron 39:951–960.

Lirk P, Poroli M, Rigaud M, Fuchs A, Fillip P, Huang CY, Ljubkovic M, Sapunar D, Hogan Q (2008) Modulators of calcium influx regulate membrane excitability in rat dorsal root ganglion neurons. Anesth Analg 107:673–685.

Lüscher C, Streit J, Lipp P, Lüscher HR (1994) Action potential propagation through embryonic dorsal root ganglion cells in culture. II. Decrease of conduction reliability during repetitive stimulation. J Neurophysiol 72:634–643.

Lüscher C, Lipp P, Lüscher HR, Niggli E (1996) Control of action potential propagation by intracellular Ca2+ in cultured rat dorsal root ganglion cells. J Physiol 490:319–324.

Ma C, Shu Y, Zheng Z, Chen Y, Yao H, Greenquist KW, White FA, LaMotte RH (2003) Similar electrophysiological changes in axotomized and neighboring intact dorsal root ganglion neurons. J Neurophysiol 89:1588–1602.

Matthews EA, Dickenson AH (2001) Effects of spinally delivered N- and P-type voltage-dependent calcium channel antagonists on dorsal horn neuronal responses in a rat model of neuropathy. Pain 92:235–246.

McCallum JB, Kwok WM, Sapunar D, Fuchs A, Hogan QH (2006) Painful peripheral nerve injury decreases calcium current in axotomized sensory neurons. Anesthesiology 105:160–168.

McCallum JB, Wu HE, Tang Q, Kwok WM, Hogan QH (2011) Subtype-specific reduction of voltage-gated calcium current in medium-sized dorsal root ganglion neurons after painful peripheral nerve injury. Neuroscience 179:244–255.

Meuth S, Pape HC, Budde T (2002) Modulation of Ca2+ currents in rat thalamocortical relay neurons by activity and phosphorylation. Eur J Neurosci 15:1603–1614.

Mironov SL, Juri MU (1990) Sr and Ba transients in isolated snail neurones studied with fura-2. The recovery from depolarization induced load and modulation of Ca release from intracellular stores. Neurosci Lett 112:184–189.

Morel N, Buryi V, Feron O, Gomez JP, Christen MO, Godfraind T (1998) The action of calcium channel blockers on recombinant L-type calcium channel alpha1-subunits. Br J Pharmacol 125:1005–1012.

Nayak AS, Moore CI, Browning MD (1996) Ca2+/calmodulin-dependent protein kinase II phosphorylation of the presynaptic protein synapsin I is persistently increased during long-term potentiation. Proc Natl Acad Sci U S A 93:15451–15456.

Patil PG, Brody DL, Yue DT (1998) Preferential closed-state inactivation of neuronal calcium channels. Neuron 20:1027–1038.

Pitt GS, Zühlke RD, Hudmon A, Schulman H, Reuter H, Tsien RW (2001) Molecular basis of calmodulin tethering and Ca2+-dependent inactivation of L-type Ca2+ channels. J Biol Chem 276:30794–30802.

Raman IM, Bean BP (1999) Ionic currents underlying spontaneous action potentials in isolated cerebellar Purkinje neurons. J Neurosci 19:1663–1674.

Randall A, Tsien RW (1995) Pharmacological dissection of multiple types of Ca2+ channel currents in rat cerebellar granule neurons. J Neurosci 15:2995–3012.

Rycroft BK, Vikman KS, Christie MJ (2007) Inflammation reduces the contribution of N-type calcium channels to primary afferent synaptic transmission onto NK1 receptor-positive lamina I neurons in the rat dorsal horn. J Physiol 580:883–894.

Saitoh T, Schwartz JH (1985) Phosphorylation-dependent subcellular translocation of a Ca2+/calmodulin-dependent protein kinase produces an autonomous enzyme in Aplysia neurons. J Cell Biol 100:835–842.

Sakaba T, Neher E (2001) Quantitative relationship between transmitter release and calcium current at the calyx of held synapse. J Neurosci 21:462–476.

Sapunar D, Ljubkovic M, Lirk P, McCallum JB, Hogan QH (2005) Distinct membrane effects of spinal nerve ligation on injured and adjacent dorsal root ganglion neurons in rats. Anesthesiology 103:360–376.

Sarantopoulos CD, McCallum JB, Rigaud M, Fuchs A, Kwok WM, Hogan QH (2007) Opposing effects of spinal nerve ligation on calcium-activated potassium currents in axotomized and adjacent mammalian primary afferent neurons. Brain Res 1132:84–99.

Scholz A, Gruss M, Vogel W (1998) Properties and functions of calcium-activated K+ channels in small neurones of rat dorsal root ganglion studied in a thin slice preparation. J Physiol 513:55–69.

Scroggs RS, Fox AP (1992) Calcium current variation between acutely isolated adult rat dorsal root ganglion neurons of different size. J Physiol 445:639–658.

Shakiryanova D, Morimoto T, Zhou C, Chouhan AK, Sigrist SJ, Nose A, Macleod GT, Deitcher DL, Levitan ES (2011) Differential control of presynaptic CaMKII activation and translocation to active zones. J Neurosci 31:9093–9100.

Stoney SD Jr (1990) Limitations on impulse conduction at the branch point of afferent axons in frog dorsal root ganglion. Exp Brain Res 80:512–524.

Swartz KJ (1993) Modulation of Ca2+ channels by protein kinase C in rat central and peripheral neurons: disruption of G protein-mediated inhibition. Neuron 11:305–320.

Swensen AM, Bean BP (2003) Ionic mechanisms of burst firing in dissociated Purkinje neurons. J Neurosci 23:9650–9663.

Ward L, Wright E, McMahon SB (1996) A comparison of the effects of noxious and innocuous counterstimuli on experimentally induced itch and pain. Pain 64:129–138.

Wu HE, Gemes G, Zoga V, Kawano T, Hogan QH (2010) Learned avoidance from noxious mechanical simulation but not threshold semmes weinstein filament stimulation after nerve injury in rats. J Pain 11:280–286.

Xiao RP, Cheng H, Lederer WJ, Suzuki T, Lakatta EG (1994) Dual regulation of Ca2+/calmodulin-dependent kinase II activity by membrane voltage and by calcium influx. Proc Natl Acad Sci U S A 91:9659–9663.

Xu J, Wu LG (2005) The decrease in the presynaptic calcium current is a major cause of short-term depression at a calyx-type synapse. Neuron 46:633–645.

Yokoyama CT, Sheng ZH, Catterall WA (1997) Phosphorylation of the synaptic protein interaction site on N-type calcium channels inhibits interactions with SNARE proteins. J Neurosci 17:6929–6938.

Yokoyama CT, Myers SJ, Fu J, Mockus SM, Scheuer T, Catterall WA (2005) Mechanism of SNARE protein binding and regulation of Cav2 channels by phosphorylation of the synaptic protein interaction site. Mol Cell Neurosci 28:1–17.

Yuan W, Bers DM (1994) Ca-dependent facilitation of cardiac Ca current is due to Ca-calmodulin-dependent protein kinase. Am J Physiol 267:H982–H993.

Zamponi GW, Snutch TP (1998) Decay of prepulse facilitation of N type calcium channels during G protein inhibition is consistent with binding of a single Gbeta subunit. Proc Natl Acad Sci U S A 95:4035–4039.

Zha XM, Dailey ME, Green SH (2009) Role of Ca2+/calmodulin-dependent protein kinase II in dendritic spine remodeling during epileptiform activity in vitro. J Neurosci Res 87:1969–1979.

Zühlke RD, Pitt GS, Deisseroth K, Tsien RW, Reuter H (1999) Calmodulin supports both inactivation and facilitation of L-type calcium channels. Nature 399:159–162.

Zühlke RD, Pitt GS, Tsien RW, Reuter H (2000) Ca2+-sensitive inactivation and facilitation of L-type Ca2+ channels both depend on specific amino acid residues in a consensus calmodulin-binding motif in the(alpha)1C subunit. J Biol Chem 275:21121–21129.